# Characterization of polyaniline/cellulose acetate nanocomposite fabricated through electrospinning

Jeanette O. Grande<sup>1</sup>', Ronniel D. Manalo<sup>1</sup>, Joybel G. Bugna<sup>2</sup>, Johanna Marie R. Dikitanan<sup>3</sup>

<sup>1</sup>Department of Forest Products and Paper Science, College of Forestry and Natural Resources, University of the Philippines Los Baños, College, Laguna, Philippines; \*Email: jogrande@up.edu.ph

**ABSTRACT.** The demand for fiber-based electronic devices or electronic textiles is on the rise. Research interest and trends are leading towards conductive nanofibers. This study dealt with the fabrication of conductive polyaniline/cellulose acetate (PANI/CA) nanocomposite through electrospinning. Polyaniline was added to cellulose acetate dissolved in dimethylformamide/acetone at different concentrations. Electrospinning was done with varying flow rates. The composition and conductivity of the nanocomposites were characterized using fourier transform infrared (FTIR) spectroscopy and four-point probe test, respectively. The fiber diameter was measured and the bead formation was assessed using scanning electron microscopy (SEM). Embedment of polyaniline in cellulose acetate was proven with the presence of characteristic peaks in the FTIR spectra. Fibers electrospun using 0.1% polyaniline at 2 mL h<sup>-1</sup> registered the highest conductivity at  $0.005416 \pm 0.000454 \text{ S m}^{-1}$ . Finest fibers with an average diameter of 91.56 nm were also obtained using the same combination. The percentage area covered by beads decreases as the PANI concentration increases and is lower at 4 mL h<sup>-1</sup>. Statistical analysis showed that PANI concentration affects the conductivity more than the electrospinning flowrate and the interaction of flowrate and PANI concentration.

**Keywords:** bead formation, conductivity, electronic textiles, fiber diameter, PANI/CA nanocomposite, spectroscopy

#### INTRODUCTION

In recent years, research on "smart materials" started to flourish as these can interact and respond to external stimuli (Kohler 2013). Among these materials, flexible electronic devices are one of the demands of this generation; thus, the birth of fiber-based electronic devices, also known as electronic textiles (Montelisciani *et al.* 2014). Depending on electrical conductivity, electronic textiles have a very wide variety of applications. These can be used for clothing to monitor the body parameters such as the rate of perspiration (Kinkeldei *et al.* 2012). These can be utilized in electrocardiogram for home healthcare purposes (Takamatsu *et al.* 2012; Kohler 2013), applied for electrically sensitive devices for antistatic purposes, and facilitation of electrostatic discharge (Bashir 2013).

To make flexible electronic devices, conductors within need to be flexible. Typical conductors such as metal oxides are vulnerable to strain failure which can typically withstand up to 2% strain only, whereas fiber-based electronic devices are resistant to up to 50% application of strain without change in its performance (Kinkeldei *et al.* 2012). Electronic textiles can also offer other desirable properties such as thermal stability and biodegradability depending on the intended purpose.

One way to engineer materials at its molecular level to achieve desirable properties is by fabrication at the nanoscale. Nanotechnology has gained interest from the scientific

<sup>&</sup>lt;sup>2</sup>Bicol Medical Center, Naga City, Camarines Sur, Philippines

<sup>&</sup>lt;sup>3</sup>Merchant Business, Inc., Florida, USA

community because of its diverse applications in different fields. Due to a significant increase in the surface area of an object at the nano level, its physical, mechanical, chemical, and optical characteristics are tremendously improved. Different techniques had been developed throughout the past decades to achieve nanoscale and one of these techniques is electrospinning.

Electrospinning is one of the newest technologies in producing superfine fibers which are within the nanoscale. The process works by allowing a solution, either in dissolved or molten form, to pass through a syringe to a metallic plate using potential difference (Cramariuc *et al.* 2013). As the solution traverses the distance from the needle to the plate, it stretches, gradually solidifies, and separates into superfine fibers. A wide range of polymers can be subjected to electrospinning (Huang *et al.* 2003).

One of the promising conducting polymers that can be administered in electrospinning is polyaniline (PANI). It is known to be a good antistatic coating due to its high chemical stability, non-toxicity, good processability, and stable intrinsic redox state (Pehkonen & Yuan 2018; Jabur 2018). Some applications of the conducting property of PANI are in ultra-sensitive hydrogen peroxide sensors, conducting gel electrolytes, dye-sensitized solar cells, polymer electrolyte membranes, and various advances (Wang *et al.* 2013; Fang *et al.* 2014; Yuan *et al.* 2014; Qui *et al.* 2014; Ansari *et al.* 2014). The synthesis of PANI is relatively simple, inexpensive, environmentally stable, and chemically durable.

To make fiber-based electrical conductors, PANI must be incorporated in a fibrous matrix. Cellulose, the most abundant naturally occurring polysaccharide, is one of the main chemical components of plant fibers. However, cellulose is difficult to electrospin without the use of strong and harmful solvents (Angel *et al.* 2020), and this problem can be solved by modification. Cellulose acetate (CA) is one of its derivatives and it has almost the same properties as cellulose itself (Edge *et al.* 1968). CA is made from the acetylation of alpha-cellulose. The porous characteristic of cellulose lends ease of manipulation of the electrons, ions, and photons (Liangbing *et al.* 2013).

PANI is an excellent electrical conductor while CA has excellent flexibility, mechanical strength, thermal stability, and biodegradability to name a few of its desirable properties. This study aims to fabricate a conducting PANI/CA nanocomposite through electrospinning, combining the desirable properties of CA while maintaining an acceptable degree of conductivity. Specifically, this study aimed to: 1) verify the embedment of PANI on CA; 2) determine the effect of PANI loading and electrospinning flowrate on the conductivity of the nanocomposites; 3) determine the effect of PANI loading and electrospinning flowrate on the average fiber diameter of the nanocomposites; and 4) determine the effect of PANI loading and electrospinning flowrate on the bead formation of the nanocomposites.

#### **METHODOLOGY**

#### Reagents

The cellulose acetate (~29,000 g mol<sup>-1</sup>) and N,N dimethyl formamide (anyhydrous, >99.8%) were obtained from Sigma–Aldrich. Acetone (>99%) was purchased from RCI Labscan Limited. Polyaniline (emeraldine salt), synthesized through chemical oxidative polymerization from aniline (>99.5%, AR), was obtained from the Physics Division, Institute of Mathematical Sciences and Physics, College of Arts and Sciences, University of the Philippines Los Baños (IMSP, CAS, UPLB).

## **Experimental design**

Polymer solutions of five different concentrations of PANI: 0.0% (pure cellulose acetate, A), 0.1% wt/v (B), 0.5% wt/v (C), 1.0% wt/v (D), and 2.0% wt/v (E) were prepared. Two variations in the electrospinning flow rate were employed: 2 mL h<sup>-1</sup> and 4 mL h<sup>-1</sup>. The effects of PANI concentration and electrospinning flow rate on the conductivity and fiber morphology were investigated. Only representative treatments were subjected to Scanning Electron Microscopy (SEM) imaging for the morphological assessment. These treatments were: A, B, and E.

#### Preparation of the PANI/CA solution

Cellulose acetate was dissolved in dimethylformamide (DMF)/acetone (3:1 v/v). The concentration of the CA–DMF/ acetone was fixed at 10% wt/v. Continuous agitation was employed until a transparent solution was achieved. In this prepared solution, different concentrations of PANI were added (**Figure 1**).

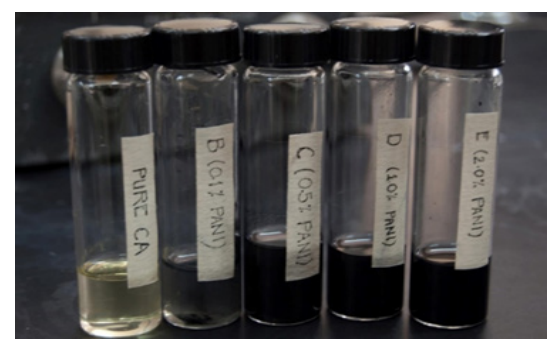


Figure 1. Different concentrations of PANI in CA-DMF/acetone solution.

## Homogenization of the solutions

The CA-DMF/acetone solutions with different PANI concentrations were homogenized through an ultrasonic bath (Cole-Parmer 08895–18) operated at 42 kHz for 90 mins. The temperature was maintained below 30°C using continuous refrigerated cycling water and checked every 15 mins of sonication time.

## **Electrospinning**

**Figure 2** illustrated the set-up for electrospinning. The solutions were fed into the syringe. As the solution traversed the distance between the syringe and the collecting screen, the solvent gradually volatilized and the PANI/CA nanocomposite fibers were collected on the aluminum sheet.

Electrospinning was performed with a fixed applied voltage of 20 kV. The distance between the syringe and the metal collector was maintained at 15 cm. The height of the metal collector was limited to 15 cm from the base. A 10 mL syringe was utilized with a controlled flow rate of 2 mL h<sup>-1</sup> and 4 mL h<sup>-1</sup>. Butterfly extensions with a gauge of 23 were used to connect the syringe in the syringe pump to the electrospinning containment. The aluminum sheet was 10 cm both in length and width.

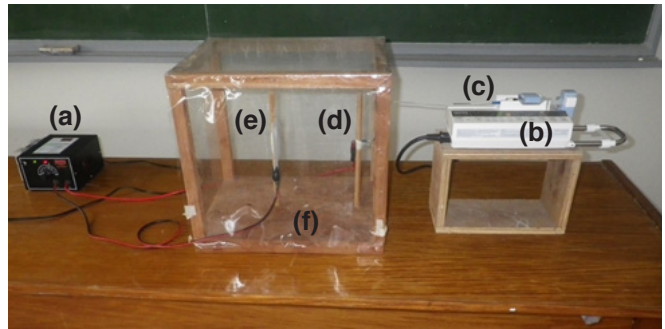


**Figure 2.** Electrospinning set-up: (a) high voltage source; (b) syringe pump; (c) syringe; (d) needle; (e) metal collector; and (f) electrospinning containment.

#### **Conductivity test**

The Four-Point Probe Test determined the conductivity of the electrospun nanocomposites. Figure 3 shows the samples for the conductivity test while Figure 4 illustrates the set-up for the conductivity test. Conductivity was determined using the following equation:

Equation 1

$$\sigma = \frac{1}{\rho} = \frac{1}{\left[\frac{2 \cdot \pi \cdot \left(\frac{V}{I}\right)}{\left(\frac{1}{S_1}\right) + \left(\frac{1}{S_2}\right) - \left(\frac{1}{S_1 + S_2}\right) - \left(\frac{1}{S_2 + S_3}\right)\right]}$$

Where V = voltage drop (V)

I = current(A)

S = distance between the probe points = 2.5 mm

 $\rho = \text{resistivity } (\Omega \cdot \mathbf{m})$ 

 $\sigma = \text{conductivity (S/m)}$ 

Since S1 = S2 = S3, then Equation 3-1 can be simplified to Equation 2.



Figure 3. Samples (2.54 cm  $\times$  2.54 cm) for the four-point probe test for conductivity.

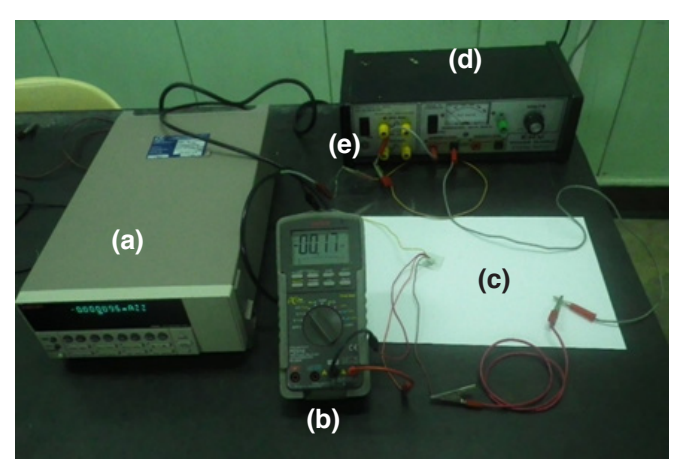


**Figure 4**. Four-point probe conductivity test set-up: (a) picoammeter; (b) multimeter (voltmeter); (c) 2.54 cm x 2.54 cm sample; (d) voltage source; and (e) resistor.

Equation 2

$$\sigma = \frac{1}{\rho} = \frac{1}{\left[2 \cdot \pi \cdot \left(\frac{\mathbf{V}}{\mathbf{I}}\right) \cdot \mathbf{S}\right]}$$

#### Morphology and composition characterization

SEM was used to measure the fiber diameter and assess the bead formation of the composite. ImageJ Version 1.47 was used to process the SEM micrographs at 5000x magnification. The summation of the area covered by individual beads was taken. Samples were subjected to Fourier Transform Infrared Spectroscopy (FTIR) to verify the presence of polyaniline in cellulose acetate.

#### Statistical analysis

The significance of the differences in conductivity results was analyzed using One-Way Analysis of Variance (ANOVA) at a 95% level of confidence. Treatment means were separated using Tukey HSD Post-Hoc Test taking into consideration the effects of the flow rate, concentration, and the interaction of flow rate and concentration. STATISTICA '97 was used for statistical analyses.

#### **RESULTS AND DISCUSSION**

# Effects of factors on the conductivity of fabricated PANI/CA nanocomposite fibers

Conducting polyaniline-cellulose acetate (PANI/CA) was fabricated using electrospinning. The highest conductivity recorded was 0.005416  $\pm$  0.000454 S m $^{-1}$  obtained from Solution B (0.1% PANI wt/v) electrospun with a solution flow rate of 2 mL h $^{-1}$ . The lowest conductivity noted on the other hand was 0.000000  $\pm$  0.000000 S m $^{-1}$  which was produced from both the control solutions (0.0% PANI wt/v) and Solution E (2.0% PANI wt/v) electrospun with both solution flow rates of 2 mL h $^{-1}$  and 4 mL h $^{-1}$ .

ANOVA was used to determine the effects of flowrate, PANI concentration, and interaction on the conductivity of PANI/CA nanocomposite at a 95% confidence level. **Table 1** summarizes the effects of the factors and interactions on the conductivity of the PANI/CA nanocomposite.

**Table 1.** Summary of effects of the flowrate and PANI concentration and their interaction on the conductivity of the PANI/CA nanocomposite.

Factor	p-level	Remarks
Flowrate	0.003244	Highly significant
PANI concentration	0.000000	Very highly significant
Flowrate X concentration	0.006053	Highly significant

#### Effect of PANI loading on conductivity

The average conductivity of the collected electrospun PANI/CA composite fibers was quantified using the four-point probe test. The conductivities of the electrospun fibers at 2 mL h<sup>-1</sup> and that at 4 mL h<sup>-1</sup> have similar trends (**Figure 5**). As the PANI loading increases, the average conductivity also increases to a certain peak and then eventually decreases. The decrease in conductivity as the concentration of PANI is increased after the peak can be attributed to the structural aggregation of PANI. As the PANI loading is

increased, the cohesive forces between its molecules increase such that larger aggregates form, consequently reducing the inter-particle contact between its molecules essential for effective conduction of electricity (Kazim *et al.* 2011).

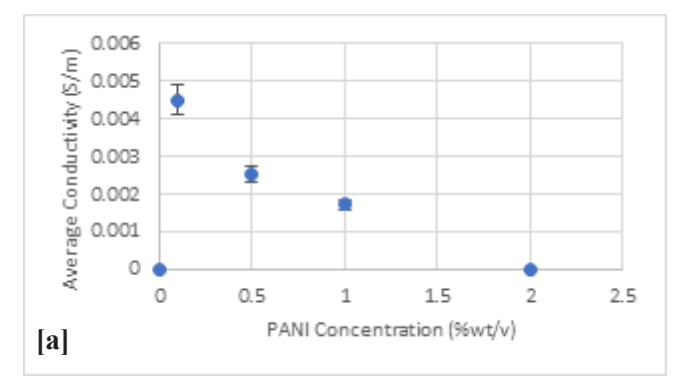
The electrical conductivity of pure cellulose acetate is 1.8 x 10<sup>-8</sup> S m<sup>-1</sup> (Kamal *et al.* 2014) while the conductivity of PANI may vary depending on the method of synthesis. Chemical oxidative polymerization was used to synthesize the polyaniline used in the experiment. Vijayanand *et al.* (2011) measured 27 S m<sup>-1</sup> using this method of synthesis. The conductivities of the nanocomposite fibers are expected between that of the conductivity of pure PANI and pure CA. The conductivity values of the fabricated nanocomposites can be used for electrostatic discharge and antistatic applications with a criterion of 10<sup>-6</sup> S m<sup>-1</sup> (Bashir 2013; Luong *et al.* 2013). Though the effectivity of e-textiles for their respective purposes is greatly dependent on the weaving technique, the conductivity recorded suffices the requisite to make electronic "smart" textiles (Yamashita *et al.* 2012; Kohler 2013).

The effect of PANI concentration on the conductivity is very highly significant (**Table 1**). Therefore, the solution concentration needs to be optimized in electrospinning the polyaniline and cellulose acetate to yield desirable electrical properties. Moreover, Tukey HSD Post-Hoc Test revealed that the average conductivity of the composite fibers from the different solutions is significantly different from each other, except that of samples A and E (**Table 2**).

Table 2. Tukey HSD post-hoc test on concentration\*.

PANI concentration (% wt/v)	Average conductivity (S m <sup>-1</sup> )
A [0.0%]	0.00000000a
B [0.1%]	0.004956163d
C [0.5%]	0.002521723c
D [1.0%]	0.001982297b
E [2.0%]	0.000000000a

\*In a column, means followed by the same letter  $\,$  are not significantly different at p <0.05



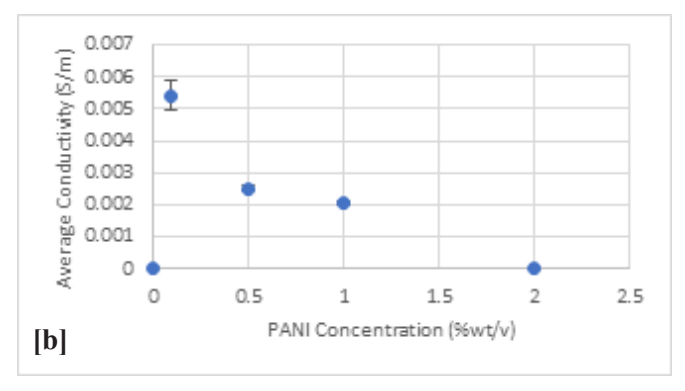
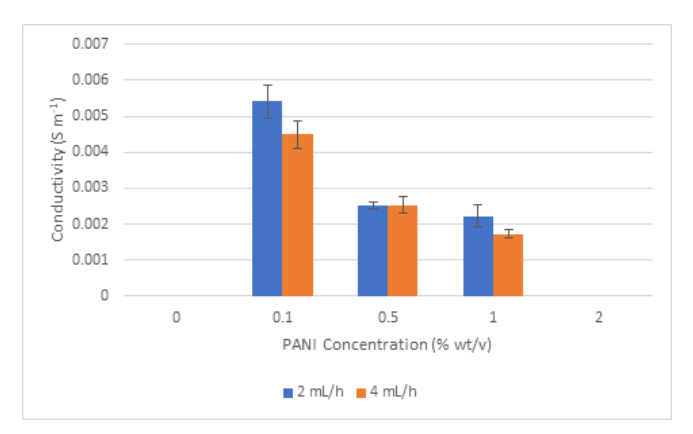


Figure 5. Average conductivity of PANI/CA nanocomposite fibers electrospun at [a] 2 mL h<sup>-1</sup> and [b] 4 mL h<sup>-1</sup>.

## Effect of flowrate on conductivity

PANI/CA nanocomposite fibers spun at 2 mL h<sup>-1</sup> solution flowrate, in general, has higher conductivity compared to those spun at 4 mL h<sup>-1</sup> (**Figure 6**).



**Figure 6.** Comparison of the average conductivity of PANI/CA nanocomposite fibers electrospun at 2 mL h<sup>-1</sup> and 4 mL h<sup>-1</sup>.

At higher flow rates, lesser negative charges migrate into the tip of the needle and therefore the solution carries an excess of positive charges at the instance it reaches the orifice to form the Taylor cone. Consequently, the volume charge decreases in the jet during electrospinning. As a result, the collected fibers electrospun at higher flowrates are less electrically conductive compared to that electrospun at lower flowrates (Theron *et al.* 2004).

The pore sizes increase at electrospinning the solution at higher flow rates (Megelski *et al.* 2002; Sill & Recum 2008). Composite fibers electrospun at higher flow rates reach the metal collector may not solidify completely, resulting to larger pores and beads in the collected nanofibers. Pores obstruct the continuity of the fibers and consequently, the inter-particle contact of the nanocomposite material decreases thereby affecting the conductivity of the material.

The electrospinning solution flowrate has a significant effect on the average conductivity of the PANI/CA composite fibers (**Table 1**). The average conductivity of the composite fibers which resulted from varying the solution flow rates significantly differs from each other (**Table 3**). This indicates that flow rate is an important process parameter to be considered in the fabrication of conducting polyaniline/ cellulose acetate nanocomposite through electrospinning.

Table 3. Tukey HSD post-hoc test on flow rate\*.

Flowrate [mL h <sup>-1</sup> ]	Mean
2	0.001752a
4	0.002032b

<sup>\*</sup>In a column, means followed by the same letter are not significantly different at p<0.05.

# Effects of factors on average fiber diameter of fabricated PANI/CA nanocomposite fibers

### Effect of PANI loading on average fiber diameter

The fibers obtained from solutions with lower concentrations have smaller average diameters compared to those with higher PANI concentrations. The smallest average fiber diameter was obtained from electrospinning solution B (0.1% PANI wt/v) at a flow rate of 2 mL h<sup>-1</sup>. On the other hand, the largest average fiber diameter was obtained from electrospinning solution E (2% PANI wt/v) at a flow rate of 2 mL h<sup>-1</sup>. There is limited data to conclude with certainty, but **Figure 7** conforms to the observation of Cramariuc *et al.* (2013) that as the solution conductivity increases with other parameters held constant, the average fiber diameter is decreased up to a certain extreme and then rises again after the minima. In the presence of a strong electric field, highly conductive solutions are very unstable leading to intense bending instability and broad diameter distribution.

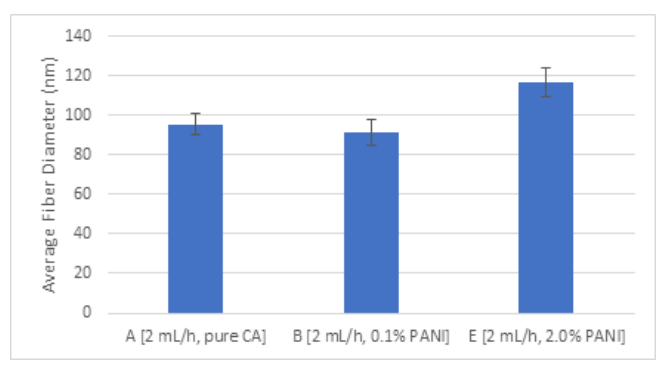


**Figure 7.** The average fiber diameter of the PANI/CA nanocomposites with different PANI loadings.

Cramariuc *et al.* (2013) devised an equation to calculate the theoretical fiber diameter emphasizing the effect of conductivity of the solution.

Equation 4-1

$$h = \left(\frac{\rho Q^3}{2\pi^2 \cdot \frac{U^2}{RZ}}\right)^{\frac{1}{4}} \cdot Z^{\frac{-1}{4}}$$

where:

h jet radius (m)

 $\rho$  density (kg/m3)

Q flowrate (m3/s)

U applied voltage (V)

Z distance from the nozzle to the collector (m)

RZ resistivity of the solution ( $\Omega$  m)

As the conductivity of the solution decreases toward zero, that is, the resistivity increases toward infinity, the fiber diameter increases toward infinity. An increase in the concentration of polyaniline in the solution, thereby increasing the conductive material, decreases the fiber diameter. Also, charge carrying capacity plays an important role. The solution with high conductivity has a greater charge carrying capacity than that of the solution with low conductivity. When exposed to an electric field, the fiber jet produced from the highly conductive solution will experience greater tensile force; consequently, producing fibers with a smaller average diameter (Pillay *et al.* 2012).

# Effect of flowrate on average fiber diameter

The average fiber diameter electrospun from pure CA at 2 mL  $h^{-1}$  was insignificantly smaller compared to that electrospun at 4 mL  $h^{-1}$ . The average fiber diameter of the nanocomposite fibers electrospun at 2 mL  $h^{-1}$  is 95.38  $\pm$  38.35 nm while that of the nanocomposite fibers electrospun at 4 mL  $h^{-1}$  is 101.94  $\pm$  63.33 nm.

Electrospinning is a process where the equilibrium of Taylor cone is important to produce uniform fibers in terms of morphology. A minimum amount of solution should be suspended at the tip of the metal spinneret to maintain this equilibrium. Varying the feed flow rate results in differences in the morphological structures of the electrospun nanocomposite fibers (Zong et al. 2002). At higher flow rates, the replacement of the solution lost when the jet is ejected is faster, not giving ample time for the Taylor cone to stabilize which causes high variation in the diameter. Additionally, as the flow rate is increased a greater volume of the solution is available in the Taylor cone and consequently, in the jet. The collected nanocomposite fiber is relatively larger in diameter and has greater pore sizes (Megelski et al. 2002).

# Effects of factors on bead formation on fabricated PANI/CA nanocomposite fibers

Beads are considered defects in nanofibers since these are points of mechanical weakness along the fiber length. **Tables 4** and **5** show the total area that the beads cover in the SEM image at 5000x magnification.

#### Effect of PANI loading on bead formation

Conductive solutions are very unstable when subjected to strong electric fields. The instability of the Taylor cone in the presence of strong electric fields causes the formation of beaded fibers. Beads can be eliminated when the net charge density balances the surface tension in the polymer solution to produce smooth, uniform non-beaded nanofibers.

As the relative concentration of PANI increases, the size of the beads decreases evidently from the percentage area of the beads. The higher the frequency of bead formation, the smaller its diameter and percentage area occupied. Nanofibers electrospun from the solution of pure CA has the lowest frequency of beads but has the highest area percentage of beads, reflecting the sizes of the beads. The nanofibers electrospun from Solution B has the highest frequency of bead formation but has the smallest area percentage of beads.

**Table 4.** Percentage area of beads of the PANI/CA nanocomposite fibers electrospun from different PANI concentrations.

PANI concentration (%wt/v)	Percentage area of beads (%)
A [pure CA]	38.81782 ± 8.58739
B [0.1%]	$30.49617 \pm 3.70396$
E [2.0%]	28.39933 ± 4.10031

#### Effect of flowrate on bead formation

The effect of flowrate on the beading formation lies in the rate of volatilization of solvent during the electrospinning process. At very high flow rates, the solvent does not vaporize completely yet before reaching the metal collector; thus, the nanofibers do not dry completely resulting in beading defects (Megelski *et al.* 2002; Pillay *et al.* 2012). Optimization of the flow rate is needed to minimize beading effects.

The sizes of the beads decrease as the flow rate increases, as shown from the values of the percentage area of the beads with respect to the image. In general, this observation in the experiment does not conform to the generalization published about electrospinning different polymers. From other researches and studies, the fiber beads increase in size. with increase in flow rate. This statement was supported by the reasoning that at a higher feeding flow rate, the droplet suspended at the tip of the metal spinneret is larger. Consequently, the jets ejected are being carried away faster and therefore relatively harder to dry before reaching the metal collector (Zong et al. 2002; Sill & Recum 2008).

Nevertheless, as presented by Megelski *et al.* (2002) in their study on the effects of flowrate on the fiber diameter and bead formation in electrospinning tetrahydrofuran (THF), a minimum flow rate is required to be determined as the optimum operating flowrate of the electrospinning process to attain minimal beading effects. Beyond that required minimum, an increase in the feeding flow rate would result in larger beads. This result was supported by Theron *et al.* (2004), accounting for the drastic decrease of volume charge density as the flow rate is decreased. They stated that the "reduction of the electric volume charge density allowed for the merging of different sections of the fiber in flight, thus facilitating the formation of garlands or beads."

The relative sizes of the beads from the nanofibers electrospun at 2 mL  $h^{-1}$  are larger than that of the nanofibers electrospun at 4 mL  $h^{-1}$ . Therefore, electrospinning the PANI/CA solutions follow the latter explanation that is, the jet ejected at a flow rate of 4 mL  $h^{-1}$  carries a higher electric volume charge that facilitates Coulombic repulsion between charges prevents the merging of the different sections of the fiber in flight compared to that of the jet ejected at a flow rate of 2 mL  $h^{-1}$ . Further validation should be done to investigate if the increase in the flow rate of the electrospinning process beyond 4 mL  $h^{-1}$  will yield larger beads conforming to the phenomena governed by the volume of the solution suspended at the tip of the spinneret.

**Table 5**. Percentage area of beads of pure CA fibers electrospun at different flow rates.

Flowrate (mL h <sup>-1</sup> )	Percentage area of beads (%)
2	38.81782 ± 8.58739
4	$22.73613 \pm 3.79000$

# FT-IR spectroscopy analysis of PANI/CA nanocomposite

Figures 8 and 9 illustrate the structural compositions of both pure PANI and CA, respectively. The stacked spectra of pure cellulose, pure PANI, and nanocomposite material collected from electrospinning solution B (0.1% PANI wt/v) at 2 mL h<sup>-1</sup> are shown in **Figure 10**. The stacked spectra show that there is a change in the peak at approximately 2940 cm<sup>-1</sup>. This frequency region corresponds to the C-H stretching in the aromatic bond which is found in PANI (Trchova & Stejskal 2011; Vijayanand et al. 2011). At 1540 cm<sup>-1</sup> there is no peak found in the spectrum of pure cellulose acetate but there is one in both the PANI and the PANI-CA nanocomposite. This is the absorbance region for the quinone ring which is a characteristic functional group of the structure of PANI (Trchova et al. 2004). The peaks that are present at the region of 1500 cm<sup>-1</sup> represent the benzene ring, also a functional group present in polyaniline but not in cellulose acetate. Additionally, the peak at 950 cm<sup>-1</sup> corresponds to the N-H bond, also a characteristic functional group of PANI (Trchova et al. 2004). The appearance of a spectra peak of the PANI-CA nanocomposite at 750 cm<sup>-1</sup> links to a substituted benzene ring (Vijayanand et al. 2011). Lastly, the peak present in the PANI/CA nanocomposite at 460 cm<sup>-1</sup> is a characteristic of the functional group SO<sub>4</sub><sup>2-</sup> (Trchova &

Stejskal 2011). Although not present in either pure PANI or CA, ammonium persulfate was used to synthesize the PANI used in this study and must have been in the PANI in small amounts; thus a proof that PANI was present in the cellulose acetate.

Figure 8. Structure of polyaniline (emeraldine salt).

Figure 9. Structure of cellulose acetate.

The peaks corresponding to polyaniline in the spectra of PANI/CA nanocomposite are minimal in magnitude. The peak intensity is proportional to the magnitude of the concentration (Smith 1999). Only minute amounts have been incorporated in the solutions.

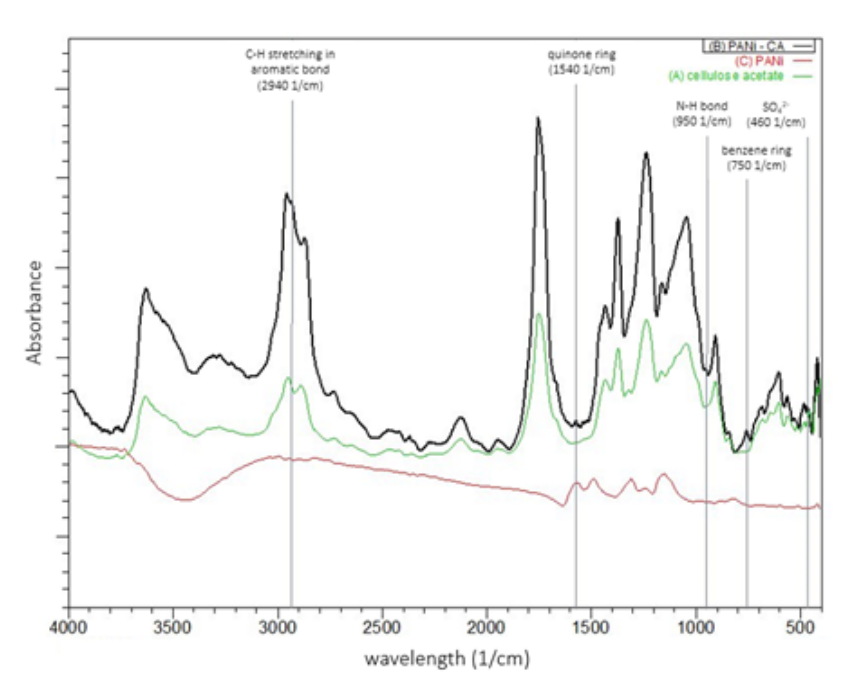


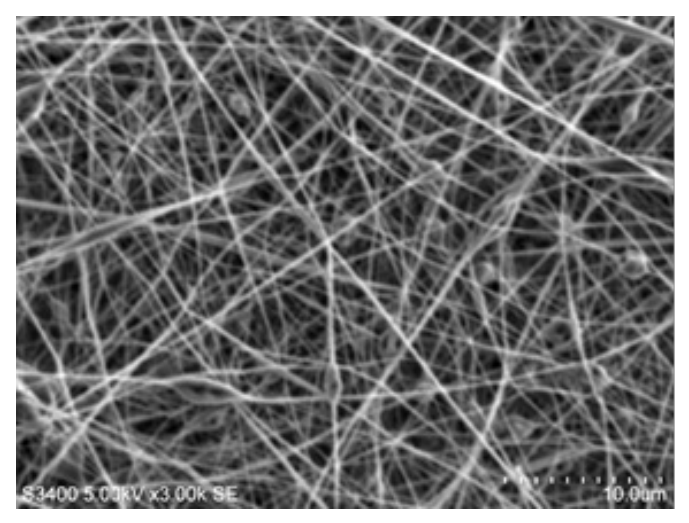
**Figure 10.** Stacked FTIR spectra of pure CA, PANI/CA nanocomposite electrospun from solution B (0.1% PANI, wt/v) at 2 mL h<sup>-1</sup>, and pure PANI.

# Morphological characterization of PANI/CA nanocomposites

The SEM images of the nanofibers electrospun from the control solution and the 2.0% solution are shown in Figure 11. There were no PANI macroparticles scattered across the fiber mats in solution E (2.0% PANI) which indicates that PANI was completely embedded in the CA nanofibers. Polyaniline was completely soluble in the DMF/acetone in the polymer solution. For a continuous fiber to be formed, a critical concentration of the polymer matrix needs to be met to provide enough chain entanglement that is necessary to provide surface tension which will balance the forces caused by the applied potential difference. In terms of fiber diameter, the treatments with no PANI or with lower PANI loading (A and B) have smaller diameters while those treatments with PANI (B and E) have a smaller percentage area of beads. Combining the factors of these variables, treatment B (0.1% PANI wt/v) exhibited the best characteristics.

## **CONCLUSION AND RECOMMENDATIONS**

Conducting PANI/CA nanocomposites were fabricated by electrospinning using different concentrations of PANI-CA solutions at different flow rates. The detection of the characteristic functional groups of polyaniline in the nanocomposite proved that PANI is present in the nanocomposite. SEM showed that PANI was not scattered in the fiber mats, thus must be embedded in the fiber structure. Further electron imaging is needed for verification. The average conductivity increases to a certain peak and then eventually decreases as the PANI loading increases. PANI/ CA composite fibers spun at 2 mL h<sup>-1</sup>, in general, has higher conductivity over the PANI/CA composite fibers spun at 4 mL h-1. As PANI loading is increased, the average fiber diameter decreased up to certain extrema and then rises again. The average fiber diameter electrospun at 2 mL h<sup>-1</sup> is smaller compared to that electrospun at 4 mL h<sup>-1</sup>. Bead formation was also considered as a factor for assessing the morphological characteristics of the PANI/CA nanocomposites.



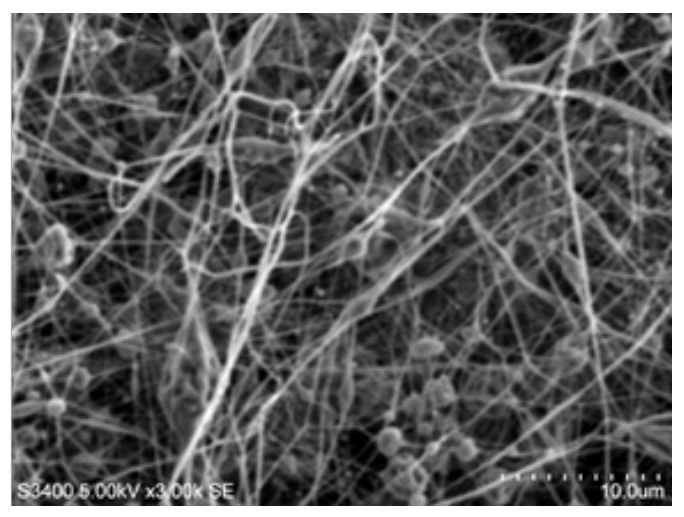


Figure 11. SEM image of nanofibers electrospun from the Solution A at 2 mL h<sup>-1</sup> [left] and from Solution E at 2 mL h<sup>-1</sup> [right].

As PANI loading increases, the size of the beads decreases as reflected from the percentage area of the beads. Bead formation increases as PANI loading increases until it reaches a certain extreme and then eventually decreases again. The sizes of the beads electrospun at 2 mL h<sup>-1</sup> were larger than that of electrospun at 4 mL h<sup>-1</sup>. Electrospinning flowrate and the interaction of flowrate and PANI concentration have highly significant effects on the conductivity of the nanocomposite while the PANI concentration has a very highly significant effect on the conductivity of the nanocomposite.

#### LITERATURE CITED

Angel, N., Guo, L., Yan, F., Wang, H., & Kong, L. (2020) Effect of processing parameters on the electrospinning of cellulose acetate studied by response surface methodology. *Journal of Agriculture and Food Research* 2: 100015.

Ansari, R.K., Price, W.E., & Wallace, G.G. (2003) Quartz crystal microbalance studies of the effect of solution temperature on the ion-exchange properties of polypyrrole conducting electroactive polymers. *Reactive and Functional Polymers* 56(3): 141–146.

Bashir, T. (2013) Conjugated Polymer-based Conductive Fibers for Smart Textile Applications. Unpublished Doctoral Dissertation – Chemical Engineering. Department of Chemical and Biological Engineering, Chalmers University of Technology, Goteberg, Sweden.

Cramariuc, B., Cramariuc, R., Scarlet R., Manea, L.R., Lupu, I.G., & Cramariuc, O. (2013) Fiber diameter in electrospinning process. *Journal of Electrostatics* 71: 189–198.

Edge, D., Jr., Fahey, M.D., & Rickey, R.G. (1968) *Acetylation of Cellulose*. Patent US3403145.

- Fang, K.C. (2014) Realization of an ultra-sensitive hydrogen peroxide sensor with conductance change of horseradish peroxidase-immobilized polyaniline and investigation of the sensing mechanism. *Biosensors and Bioelectronics* 55; 294–300.
- Huang, Z.M., Zhang, Y.Z., Kotaki, M., & Ramakrishma, S. (2003) A review on polymer nanofibers by electrospinning and their applications in nanocomposites. *Composites Science and Technology* 63: 2223–2253.
- Jabur, A.R. (2018) Effect of polyaniline on the electrical conductivity and activation energy of electrospun nylon films. *International Journal of Hydrogen Energy* 43: 530–536.
- Kamal, H., Abd-Elrahim, F.M., & Lotfy, S. (2014) Characterization and some properties of cellulose acetate-co-polyethylene oxide blends prepared by the use of gamma irradiation. *Journal of Radiation Research and Applied Sciences* 7: 146–153.
- Kazim, S., Ahmad, S., Pfleger, J., Pleastil, J., Joshi, Y.M. (2011) Polyaniline–sodium montmorillonite clay nanocomposites: effect of clay concentration on thermal, structural, and electrical properties. *Journal of Materials Science* 47: 420–428.
- Kinkeldei, T., Zysset, C., Munzenrieder, N., & Troster, G. (2012) An electronic nose on flexible substrates integrated into a smart textile. *Sensors and Actuators B: Chemical* 174: 81–86.
- Kohler, A.R. (2013) Challenges for eco-design of emerging technologies: The case of electronic textiles. *Materials and Design* 51: 51–60.
- Liangbing, H., Zheng, G., Yao, J., Liu, N., Eskilsson, M., Karabulut, E., Ruan, Z., Fan, S., Bloking, J.T., McGehee, M.D., Wägberg, L., & Chui, Y. (2013) Transparent and conductive paper from nanocellulose fibers. *Energy Environmental Science* 6: 513–518.
- Luong, N.D., Korhonen, J.T., Soininen, A.J., Ruokolainen, J., Johanssson, L.S., & Seppala, J. (2013) Processable polyaniline suspensions through in situ polymerization onto nanocellulose. *European Polymer Journal* 49: 335–344.
- Megelski, S., Stephens, J.S., Chase, D.B., & Rabolt, J.F. (2002) Micro- and nanostructured surface morphology on electrospun polymer fibers. *Macromolecules* 35: 8456–8466.
- Montelisciani, G., Mazzei, D., & Fantoni, G. (2014) How the next generation of products pushes to rethink the role of users and designers. *Procedia CIRP* 21: 93–98.
- Pehkonen, S.O. & Yuan, S. (2018) Conducting polymer coatings as effective barrier to corrosion. *Interface Science and Technology* 23: 23–61.

- Pillay, V., Dott, C., Choonara, Y.E. Tyagi, C., Tomar, L., Kumar, P., du Toit, L., & Nededendo, V.M.K. (2013) A review of the effect of processing variables on the fabrication of electrospun nanofibers for drug delivery applications. *Hindawi Publishing Corporations, Journal of Nanomaterials* 2013(1). <doi:10.1155/2013/789289>.
- Qiu, Y. (2014) High-performance polyaniline counter electrode electropolymerized in presence of sodium dodecyl sulphate for dye-sensitized solar cells. *Journal of Power Sources* 253: 300–304.
- Sill, T.J. & Recum, H.A. (2008) Electrospinning: Applications in drug delivery and tissue engineering. *Biomaterials* 29: 1989–2006.
- Smith, B.C. (2000) Infrared Spectral Interpretation: A Systematic Approach [Electronic version]. Florida: CRC Press LLC.
- Takamatsu, S., Kobayashi, T., Shibayama, N., Miyake, K., & Itoh, T. (2012) Fabric pressure sensor array fabricate with die-coating and weaving techniques. Sensors and Actuators A 184: 57–63.
- Theron, S.A., Zussman, E., &Yarin, A.L. (2004) Experimental investigation of the governing parameters in the electrospinning of polymer solutions. *Polymer* 45: 2017–2030.
- Ttchova, M., Sedenkova, I., Tobolkova, E., & Stejskal, J. (2004) FTIR spectroscopic and conductivity study of the thermal degradation of polyaniline films. *Polymer Degradation and Stability* 86:179–185. doi:10.1016/j.polymdegradstab.2004.04.011.
- Vijayanand, P.S., Vivekanandan, J., Ponnusamy, V., & Mahudeswaran, A. (2005) Synthesis, characterization and conductivity study of polyaniline prepared by chemical oxidative and electrochemical method. Archives of Applied Science Research 3 (6): 147–153.
- Wang, S., Lu, S., Li, X., Zhang, X., He, S., & He, T. (2013). Study of H<sub>2</sub>SO<sub>4</sub> concentration on properties of H<sub>2</sub>SO<sub>4</sub> doped polyaniline counter electrodes for dye-sensitized solar cells. *Journal of Power Sources* 242: 438–446.
- Yamashita, T., Takamatsu, S. Miyake, K., & Itoh, T. (2012) Fabrication and evaluation of a conductive polymer coated elastomer contact structure for woven electronic textile. *Sensors and Actuators A* 195: 213–218.
- Yuan, S., Tang, Q., Hu, B., Ma, C., Duan, J., & He, B. (2014) Efficient quasi-solid-state dye-sensitized solar cells employing polyaniline and polypyrrole incorporated microporous conducting gel electrolytes. *Journal of Power Sources* 254: 98–105.
- Zong, X., Kim, K., Fang, D., Ran, S., Hsiao, B.S., & Chu, B. (2002) Structure and process relationship of electrospun bioabsorbable membranes. *Polymer* 43: 4403–4412.